

Nonradiating anapole condition derived from Devaney-Wolf theorem and excited in a broken-symmetry dielectric particle

GIUSEPPE LABATE,^{1,2,*} ANAR K. OSPANOVA,³ NIKITA A. NEMKOV,⁴ ALEXEY A. BASHARIN,^{3,5} AND LADISLAV MATEKOVITS¹

¹*Department of Electronics and Telecommunications, Politecnico di Torino, Corso Duca degli Abruzzi 24, 10129 Torino, Italy*

²*Current affiliation: Wave Up S.r.l. - Innovation in Electromagnetics, via Roma 77, 53100 Siena, Italy*

³*University of Science and Technology "MISiS", The Laboratory of Superconducting Metamaterials and Department of Theoretical Physics and Quantum Technologies, Leninsky pr. 4, 119049, Moscow, Russia*

⁴*Universität zu Köln, Mathematisches Institut, Weyertal 86-90, 50931 Köln, Germany*

⁵*Scientific and Technological Center of Unique Instrumentation RAS (STC UI RAS), 117342, Butlerova str., 15, Moscow, Russia*

*giuseppe.labate@wave-up.it

Abstract: In this work, we first derive the nonradiating anapole condition with a straightforward theoretical demonstration exploiting one of the Devaney-Wolf theorems for nonradiating currents. Based on the equivalent volumetric and surface electromagnetic sources, it is possible to establish a unique compact conditions directly from Maxwell's Equations in order to ensure nonradiating anapole state. In addition, we support our theoretical findings with a numerical investigation on a broken-symmetry dielectric particle, building block of a metamaterial structure, demonstrating through a detailed multiple expansion the nonradiating anapole condition behind these peculiar destructive interactions.

© 2020 Optical Society of America under the terms of the [OSA Open Access Publishing Agreement](#)

1. Introduction: electromagnetic radiationless sources

Research works on the electrodynamics of charge-current distributions which do not radiate have started since 1900s from the interest on electron models, its radiationless orbits, electromagnetic self-force and radiation reaction [1–7]. Even if a number of nonradiating configurations have been studied, a first general technique for determining such radiationless sources has been given in 1973 by Devaney and Wolf [8], where five nonradiating theorems have been derived in order to set different configurations of nonradiating currents able to strictly localize the fields they generate. Since Devaney-Wolf pioneering work, several research efforts have been stimulated towards novel configurations of nonradiating sources and their fields [9–15]: a comprehensive review on the history of nonradiating sources, invisible objects can be found in [16,17].

In order to discriminate between all the different families of nonradiating sources, since - by definition - they do not radiate any external field outside their occupied volume, it is necessary to look at their internal field configurations, revealing radiationless sources with internal null (electric or magnetic) field [18], with internal singular field values forming embedded (optical bound) eigenstates [19] or with internal interfering electromagnetic multipoles creating nonradiating anapole modes [20–24].

Due to its peculiar features, growing research interest has been dedicated to the radiationless anapole mode, excited in different dielectric (or metal-dielectric) particles of various shapes [25–27] in order to generate simultaneously both electric dipole and toroidal dipole possessing the same angular distribution and parity properties [28]: as a consequence, the electromagnetic fields of destructively oscillating electric and toroidal dipoles disappear everywhere apart from the origin, forming the elementary anapole mode [29]. The mathematical condition relating the

electric dipole \vec{P} and the toroidal dipole \vec{T} , leading to the formation of anapole modes, has been usually derived considering the *external* far-field cancellation of the time-varying charge-current configurations, without considering a direct characterization in terms of the nonradiating electric and magnetic currents induced in the *internal* occupied volume.

Without the need to compute far-field radiation and without expanding near-field configurations in harmonic waves, it has been demonstrated by some of these authors in [30] that is possible to derive from Devaney-Wolf theorems a unified theory directly based on equivalent volumetric and surface nonradiating currents, leading to several straightforward conditions on optical invisibility [17] and devices using a metasurface/metamaterial cloaking shell [31–36]. In particular, the cloaking techniques based on Mie theory that exploit plasmonic materials [31,37] or impedance metasurface coatings [32,38–41] have been compactly demonstrated to correspond to the family of nonradiating (electric and magnetic) currents possessing zero-mean value in the volume of the particle: due to its integral formulation, this solution has been named as weak solution [30]. Other techniques based on tensor formalism and spatial transformation of the constitutive parameters ϵ and μ [33,42,43] or of the Z impedance property [44] have been compactly demonstrated to correspond to another class of nonradiating (electric and magnetic) currents having local equivalent zero value in the volume of the particle: due to its strict local validity, this solution has been named as strong solution [30]. A comprehensive summary of such unified theory in the framework of nonradiating currents has been recently reported for metamaterial and metasurface cloaking applications [45].

The nonradiating anapole mode has been *qualitatively* categorized in the class of weak solutions due to its loop-induced mode [30] and in this work we first *quantitatively* demonstrate in a straightforward manner the specific condition between \vec{P} and \vec{T} for generating the anapole mode directly from Devaney-Wolf theorems. To verify the nonradiating anapole condition, experimentally observed in 3D SRR-like structures [20] and in dielectric nanodisks [21], we verify in a broken-symmetry dielectric particle the external field to be transparent to the incoming radiation and the internal field to be expressed in terms of \vec{P} and \vec{T} through a detailed multipole expansion as investigated for other different particles by some of these authors [22,23,46]. Starting from the differential form of the Maxwell's Equations, we derive the compact condition that accurately describes the formation of the nonradiating anapole phenomenon in terms of volumetric magnetization and polarization vectors. A realistic broken-symmetry dielectric particle, exhibiting external transparency effect and internal anapole mode, is presented and numerically simulated, demonstrating the validity of the proposed paradigm.

2. Theoretical demonstration: exploiting Devaney-Wolf theorem V

In [30], some of these authors have demonstrated two classes of nonradiating sources, namely strong and weak solutions, directly from the Devaney-Wolf theorem number III, which defines a radiationless source through the zeros of its Fourier transform [8]. It is worthwhile mentioning that all five Devaney-Wolf theorems start from the considerations of *free* currents, able to evolve within the domain without considering any support from external excitations or scatterers involved in the scenario. In this work, it is tacitly assumed that there exist no free currents or charges in the domain, whereas it is of interest to explore the relation between *bound* currents existing as physically excited/induced on passive scatterers. Due to the fact that these bound currents can be separately treated from the involved dielectric or metallic materials via equivalence principles [40], it is still possible to exploit the same mathematical form of Devaney-Wolf theorems for such *equivalent* currents even if these sources possess a physical meaning behind. This appears to be as an advantage for the synthesis process of dielectric or metal-dielectric particles, as shown in the following Section about the excitation of a nonradiating source in a broken-symmetry dielectric particle.

Before exploiting one of the Devaney-Wolf theorems in [8], it is worthwhile to discuss the graphical representation of currents in Fig. 1 of any scatterer separated on the overall volume V in two subdomains: a generic cluster of volumetric scatterers - represented by V_1 , and the additional subdomain V_2 (Fig. 1(a)). The surface currents excited by the incident electromagnetic wave generate surface and volumetric currents that in turn will radiate. However, the main feature of such nonradiating configuration is related to the destructive interference between the currents \vec{J}_1 and \vec{J}_2 in the object placed in V_1 , and those currents on the properly positioned additional matter in V_2 . In case the internal element of volume V_1 supports (an electric) dipole-like response described in terms of its polarization vector \vec{P} , the additional structure of volume V_2 should produce a current distribution that will generate a similar radiation pattern. This can be performed by considering another electric dipole-like structure, ensuring their far-field radiations to possess destructive interferences between each other: this methodology has been pursued in the scattering cancellation approach [31,32]. However, higher-order current configuration, beyond the dipole-like response, can still radiate in a similar manner as the toroidal dipole, characterized by lateral poloidal currents sustaining a toridization vector \vec{T} (Fig. 1(b)) [20,28,47]. When properly excited, the two radiations (generated by \vec{P} and \vec{T}) will cancel out each other, bringing out a nonradiating configuration in the far-field.

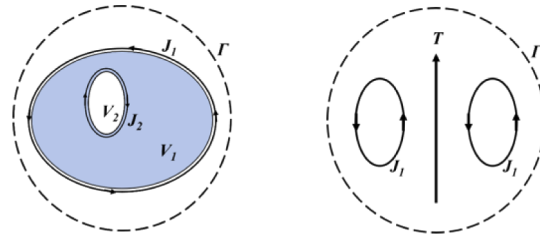


Fig. 1. Top view of volume V_1 incorporating a generic cluster V_2 of volumetric dielectric scatterer (a). Γ indicates the virtual boundary (surface) between the occupied volume V and the external space. Side view with equivalent treatment (b) with volumetric dielectric sources \vec{J}_1 and \vec{J}_2 .

Let us start from a proper manipulation of the two curl differential Maxwell's Equations, with right hand terms as equivalent sources (that in the most general case, include both surface and volumetric currents), expressed as follows

$$\nabla \times \vec{E} = -i\omega\mu_0\vec{H} \tag{1}$$

$$\nabla \times \vec{H} = i\omega\varepsilon_0\vec{E} + \vec{J}_{eq} \tag{2}$$

where the $e^{-i\omega t}$ time convention has been assumed. The equivalent electromagnetic source \vec{J}_{eq} is expressed as a combination of the electric and/or magnetic volumetric and surface current components. In particular, one can express the terms for the volumetric electric and magnetic current contributions, \vec{J}_v^e and \vec{J}_v^m , as follows [48]

$$\vec{J}_v^e(r') = +i\omega\varepsilon_0\vec{P}(r') \quad \text{with } r' \in V \tag{3}$$

$$\vec{J}_v^m(r') = -Y_0\nabla \times \vec{M}(r') \quad \text{with } r' \in V \tag{4}$$

where \vec{P} and \vec{M} are the polarization and magnetization vectors, respectively. The term $Y_0 = \sqrt{\varepsilon_0/\mu_0}$ indicates the intrinsic admittance in free-space. For the equivalent surface currents, they

have the expressions [48]

$$\vec{J}_s^e = \hat{n} \times [\vec{H}^+ - \vec{H}^-] \quad \text{with } r' \in \Gamma \quad (5)$$

$$\vec{J}_s^m = -\hat{n} \times [\vec{E}^+ - \vec{E}^-] \quad \text{with } r' \in \Gamma \quad (6)$$

The equivalent surface sources \vec{J}_s^e and \vec{J}_s^m are expressed in terms of the discontinuities of the total magnetic and electric fields, respectively, defined just outside (Γ^+) and inside (Γ^-) the contour surface Γ . In Eq. (5) and Eq. (6) \hat{n} indicates the outgoing normal unit vector to the surface Γ at the point of definition for the equivalent sources. It is worthwhile mentioning that as a function of the materials supporting the scattering phenomenon, the presence of dielectric, magnetic or conductive objects in a given vacuum scenario can be equivalently described by a combination of volumetric and surface equivalent sources. With the standard procedure to decouple the two Maxwell's equations, obtained by applying the curl operator to Eq. (1) and substituting the expression of the curl for the magnetic field using Eq. (2) (and viceversa), the expressions become:

$$\nabla \times \nabla \times \vec{E} - k_0^2 \vec{E} = -i\omega\mu_0 \vec{J}_{eq} \quad (7)$$

$$\nabla \times \nabla \times \vec{H} - k_0^2 \vec{H} = \nabla \times \vec{J}_{eq} \quad (8)$$

It is worthwhile noticing that the source terms in Eq. (7) and Eq. (8) (right-hand) are directly proportional to the equivalent sources \vec{J}_{eq} or to the curl of them. In [18], it has been highlighted that by imposing to zero the source terms on the right-hand side of decoupled Maxwell's equations, an intriguing possibility comes out: with no additional free-propagating fields in the system, there will be no source of electric waves in Eq. (7) or magnetic waves in Eq. (8), if

$$\vec{J}_{eq} = 0\vec{p} \quad \text{with } r' \in \Gamma \quad (9)$$

$$\nabla \times \vec{J}_{eq} = 0\vec{p} \quad \text{with } r' \in V \quad (10)$$

where \vec{p} is the corresponding polarization unit vector. As a consequence, similarly to the reasonings in [18] in terms of auxiliary fields, the non-trivial solutions here expressed in terms of equivalent currents, associated to the corresponding Helmholtz Eqs. (7) and (8) are of nonradiating nature since no energy outside the volume V can be released, corresponding to a possible presence of trapped energy inside V forming radiationless electromagnetic modes. The two compact conditions in Eq. (9), imposed at the boundary Γ enclosing all the scatterers, and Eq. (10), imposed in the entire volume V , generalize in their differential formalism the paradigm of strong and weak solutions, first introduced in [30]. While Eq. (10) is consistent with the result of Van Bladel [49], at a glance Eq. (9) can appear as a trivial solution if imposed in the entire volume V as in Eq. (10): it simply indicated the absence of currents within the volumetric domain. However, considering Eq. (9) to be valid at the boundary Γ , it corresponds to a non-trivial condition, since it states that it is the cancellation of equivalent electric (and magnetic) sources at Γ that determines nonappearance of scattering beyond the boundary, as the key concept demonstrated in [40]. However, here we demonstrate not only the external transparency condition but that, at the same time, the nontrivial internal field configuration corresponds to a nonradiating anapole mode. Since the anapole mode to form needs both electric and magnetic currents, let us assume only two volumetric sources according to Eqs. (3) and (4) and that, their sum, according to condition (Eq. (9)), becomes zero as

$$i\omega\varepsilon_0\vec{P} - Y_0\nabla \times \vec{M} = 0\vec{p}. \quad (11)$$

Equation (11) describes the required interaction between the polarization \vec{P} and magnetization \vec{M} vectors within a nonradiating particle. The result is consistent with the concept of null-field

radiationless source [18] and it can also explain the mechanism behind the Transformation Optics based approaches in a differential formalism [33,34]. In addition, we consider the specific presence of a toroidal dipole response within the particle as responsible for the equivalent magnetization vector \vec{M} as

$$\vec{M} = \nabla \times \vec{T} \quad (12)$$

the result in Eq. (11) takes the form of

$$\vec{J}_{eq} \equiv \nabla \times \nabla \times \vec{T} - ik_0 \vec{P} = 0\vec{p} \quad (13)$$

where the equivalent currents have been explicit as a function of \vec{T} and \vec{P} . With this formalism, it is possible to *directly* compare Eq. (13) with one of the Devaney-Wolf theorems. As reported in [8], the last of the five Devaney-Wolf theorems (number V) states that:

If \vec{F} is any vector field that is continuous and has continuous partial derivatives up to the third order and that vanishes at all points outside its finite volume, the condition

$$\vec{J}_{NR} = \frac{1}{4\pi i} \left(\frac{c}{k_0} \right) \left\{ \nabla \times \nabla \times \vec{F} - k_0^2 \vec{F} \right\} \quad (14)$$

ensures that \vec{J}_{NR} is a nonradiating current [8] in the occupied volume V , where $k_0 = \omega\sqrt{\epsilon_0\mu_0}$ denotes the free space wavenumber at the angular frequency ω and c is the speed of light.

By imposing the zero local condition of the equivalent currents in Eq. (13) and in Eq. (14), the connection between \vec{P} and \vec{T} is quantitatively estimated, by assuming $\vec{F} \equiv \vec{T}$, as

$$\vec{P} + ik_0 \vec{T} = 0\vec{p} \quad (15)$$

in order to achieve a non-radiating configuration of anapole type. As an additional proof concerning the Devaney-Wolf theorem V, once inserted Eq. (15) into Eq. (13) as a function of \vec{T} , the physics behind is the same as Eq. (14): a wave equation for the vector $\vec{F} \equiv \vec{T}$. It is worthwhile mentioning that Eq. (11), once the current sources involved in the system have been explicit as two volumetric currents, remains a *sufficient* condition, as derived from Devaney-Wolf theorems, for a current source to be nonradiating. However, Eq. (11) is *not necessary* condition since many other alternatives, depending on the topology and nature of the currents involved in the system may exist. This essential consistency and fitting between theoretical results and experimental observations of the anapole mode [20,21,25–27,29] represents an intriguing aspect of modeling the problem from the perspective of equivalent nonradiating currents: as highlighted by the formalism in Eq. (15), the derived anapole condition has to be valid for each cartesian component for the proper balancing of $\vec{P} = -ik_0 \vec{T}$ (as highlighted in the Appendix). In the next section, we numerically demonstrate further such anapole condition in Eq. (15), based on equivalent nonradiating currents.

3. Numerical demonstration: a broken-symmetry dielectric metamaterial particle

Exploiting the formalism of equivalent nonradiating currents, it has been demonstrated that, in order to sustain a radiationless configuration of anapole type, there is the need to sustain two volumetric currents. The first current has to be supported by an electric dipole response \vec{P} , thus a simple dielectric particle can be chosen to this purpose. However, since as a function of its size in terms of incoming wavelength, a dielectric particle can excite not only a pure dipole moment, but also higher order multipoles [50], the overall dimensions have to be subwavelength for the incoming fields: in quasi-static or subwavelength regime, the dominant scattered wave for a dielectric particle is a pure dipole response \vec{P} [31]. On the other hand, the second current has to be supported by a toroidal response \vec{T} and, since it is still possible to exploit the subwavelength

condition to excite a dominant electromagnetic mode, a dielectric particle with a centered-hole (similar to a torus) can serve to this purpose.

In [46] (and reference therein), it is reported that it is possible to excite anapole modes also as a combination of electromagnetic responses coming from several dielectric or metallic particles, however, in this work we introduce an example of nonradiating anapole mode due to symmetry breaking of a pseudo-toroidal structure, in order to excite both \vec{P} and \vec{T} within a single dielectric particle. Even if the toroidal response can also be excited in individual particles [21,28,46,62,63], we consider here a periodic arrangement as in metamaterials instead of a single particle, as reported in Fig. 2. The reason behind this design choice is that, with the use of a periodic system as in metamaterials, it remains possible to reduce the influence of higher-order multipoles, as quadrupoles for instance.

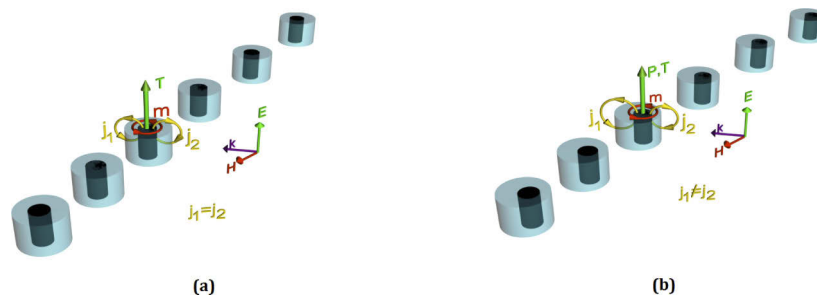


Fig. 2. Illustration of subwavelength high-index dielectric cylinders in a periodic arrangement with symmetric (a) and asymmetric (b) hole. Here \vec{J} denotes displacement currents, \vec{m} magnetic moment, \vec{P} and \vec{T} is electric and toroidal dipole moments, respectively.

Let us assume for example a gedanken torus in a periodic arrangement (infinite-height hole cylinders arranged periodically) that possesses surface poloidal currents that occur due to interaction with incident electromagnetic wave. As it can be seen from Fig. 2(a), these currents create a loop of magnetic field within the torus and the combination of these modes can sustain a toroidal response \vec{T} according to Eq. (12). The trade-off to generate within a single nonradiating particle both dipole and toroidal response is to consider a dielectric cylinder with a hole (filled by air), but shifted (not centered) with respect to the cylinder's axis. This is due to the fact that when the central axis of the formed torus is moved from its initial position, it leads to an asymmetric cross section along the torus, as shown in Fig. 2(b). Due to such symmetry breaking, the proper electromagnetic multipole fitting the toroidal geometry is not only a pure toroidization vector \vec{T} , but due to the local modification of the current paths in the meridian planes, unequal displacement currents \vec{J}_1 and \vec{J}_2 create an uncompensated electric response \vec{P} (completely absent in the initial configuration due to the complete symmetry). These electric and toroidal moments both oscillate and, at a given frequency where Eq. (15) is satisfied, a dynamic anapole mode can be established as a nonradiating state characterized by a strong field concentration within the volume of the torus.

If the symmetric structure (a purely torus with a central hole) interacts with an incident electromagnetic wave leading to a strong electromagnetic scattering, the broken-symmetry dielectric particle, with modified configurations of electric and toroidal modes, strongly suppress the electromagnetic scattering and a nonradiating state is generated when Eq. (15) is satisfied. In Fig. 2(a), we consider a metamaterial consisting of periodically arranged subwavelength high-index dielectric indefinitely elongated cylinders with a central hole, resembling a toroidal configuration. An incoming plane wave with electric component E_y , parallel to the cylinder axis, is responsible for inducing the so called magnetic Mie resonance that represents the electromagnetic response of dielectric particles in analogy with plasmonic resonance in metals [24,51,52]. This

aspect on Mie resonances, as also related to the generation of toroidal dipole response exploiting Mie theory has been deeply treated in [53] and closed-form solution have been obtained for dielectric particles in [40] and for metallic obstacles in [41]. However, since Mie theory applies only to center-symmetric structures, it can not be used to investigate with closed-form solutions the broken-symmetry dielectric particle (since it is intentionally not center-symmetric), but it can give guidelines on the physics behind it. According to Mie theory, the electromagnetic response of dielectric particle is underpinned by the displacement currents $\vec{J}_1 = \vec{J}_2$, occurring within its volume by the incident wave and these displacement currents take the form of loops, generating aligned head-to-tail magnetic modes within the hole of the cylinder. Such electromagnetic configuration resembles the surface poloidal currents and magnetic moments within a torus that, as expected, create a toroidal dipole \vec{T} oscillating along the symmetry axis [53–58].

On the other hand, if the hole is shifted from the center towards any distance d , the produced asymmetry affects the charge-current redistribution within the metamolecule, as reported in Fig. 2(b). Displacement currents \vec{J} still generate ring-like magnetic modes within the cylinder and their combination excites toroidal dipole response \vec{T} . In addition, unequal redistribution of displacement currents \vec{J}_1 and \vec{J}_2 leads to uncompensated electric response \vec{P} that becomes resonant at certain frequency. Therefore, these electric \vec{P} and toroidal \vec{T} dipole moments oscillate and there is the possibility to form a $\vec{P} + ik_0\vec{T}$ relation inducing an anapole mode establishment when it is zero, satisfying Eq. (15) and corresponding to a nonradiating state. In this example, the nonradiating particles of the metamaterial are made up of an infinitely elongated $h = \infty$ dielectric cylinders placed in a vacuum scenario. The radius of the cylinder is $R = 25\mu\text{m}$ and the hole has radius $r = 5\mu\text{m}$, considering the periodicity of a square unit cell metamolecule to be with $l = 70\mu\text{m}$. For such subwavelength particle, we simulate properties of high-index dielectrics showing a relative permittivity $\epsilon_r = 41.4$ (which is very close to the dielectric constant of LiTaO₃ in the low THz regime [53]) and we study the electromagnetic response of this structure using the commercial software CST [59] and HFSS [60] solvers, obtaining the same results for external and internal field configurations. The properly chosen parameters lead to couple magnetic Mie modes in the dielectric particle, when the cases with $d = [0, 2, 3, 3.5, 4]\mu\text{m}$ hole displacements are considered.

To study the electromagnetic response of such dielectric metamaterial, a detailed decomposition of the excited multipoles has been obtained close to resonant frequency range up to second order multipole, namely electric \vec{P} and magnetic \vec{M} dipole, toroidal \vec{T} dipole, electric \vec{Q}_e and magnetic \vec{Q}_m quadrupole moments. As expected, the centered hole position $d = 0\mu\text{m}$ corresponds to a dominating toroidal response of the system at $f = 1.215$ THz, as reported in Fig. 3(a). According to our approach, the asymmetric position of the hole with respect to the cylinder axis leads to redistribution of displacement currents \vec{J}_1 and \vec{J}_2 and, consequently, electric dipole response occurs. The gradual hole displacement for $d = 2\mu\text{m}$ and $3\mu\text{m}$, as shown in Figs. 3(b) and 3(c) manifests itself as an increase of electric \vec{P} dipole moment that approaches the toroidal \vec{T} dipole moment for $d = 3.5\mu\text{m}$ at $f = 1.215$ THz, as reported in Fig. 3(d). Eventually, electric dipole \vec{P} moment intensity exceeds toroidal dipole \vec{T} moment for $d = 4\mu\text{m}$, as shown in Fig. 3(e). Moreover, the case of $d = 3.5\mu\text{m}$ hole displacement is characterized by the overlapping of the electric and toroidal dipole moments at $f = 1.215$ THz corresponding to radiation compensation and to anapole mode establishment as detailed in Fig. 3(d). On the other hand, all cases of hole displacement are accompanied by strong magnetic response of the system that maintains constant nonresonant magnetic dipole \vec{M} contribution at any value of d at resonance frequencies.

However, the broken symmetry of particles strongly influences the electric dipole \vec{P} evolution which is negligible for $d = 0\mu\text{m}$ and it achieves toroidal dipole moment \vec{T} for anapole formation for the case when $d = 3.5\mu\text{m}$, which we choose to investigate in detail.

In order to check the validity of this approach for the external electric and magnetic field distribution at this frequency, we first analyze the electromagnetic response of a stand-alone

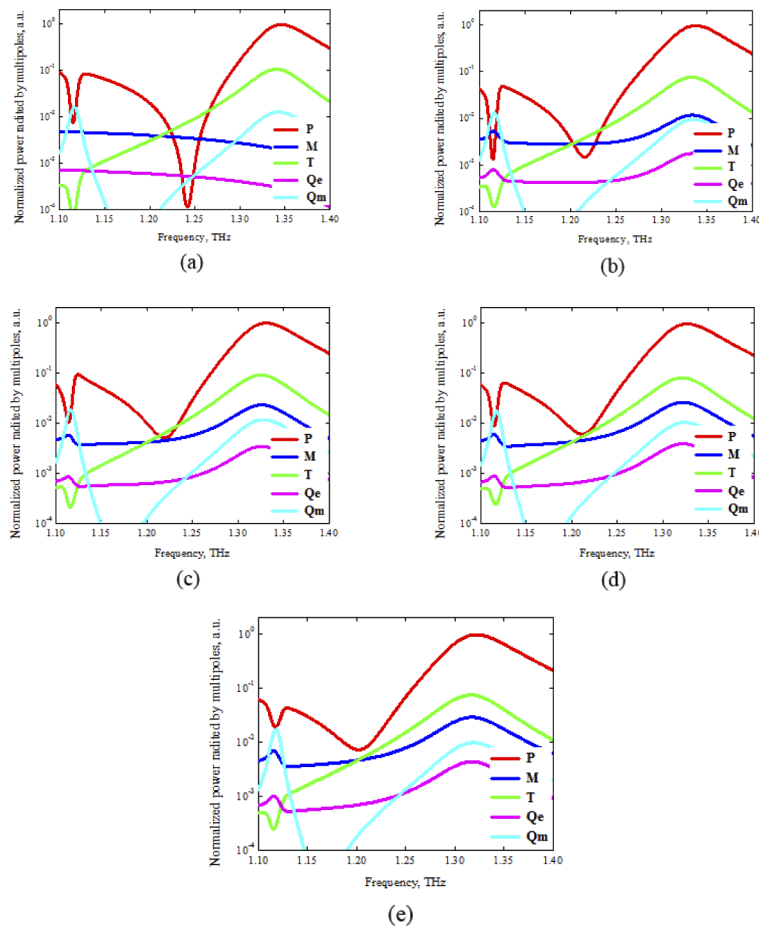


Fig. 3. Normalized power scattered by the multipoles excited in the dielectric particles at 1.1 THz-1.4 THz frequency range for $d = 0\mu\text{m}$ (a), $2\mu\text{m}$ (b), $3\mu\text{m}$, (c) $3.5\mu\text{m}$ (d) and $4\mu\text{m}$ (e) hole displacements.

dielectric particle with the broken-symmetry hole with $d = 3.5\mu\text{m}$, as in Figs. 4(a)–4(b). As expected, the incoming plane wave (coming from the left of the drawings) excites the dielectric particle generating a weak reflection and a strong transmission through the dielectric object, when crossing the broken-symmetry hole. Colorbar values are saturated to the incident field values in absence of object, with $E_0 = 1\text{ V/m}$ and $H_0 = (120\pi)^{-1}\text{ A/m}$ (due to the fact that for the incident field is $H_0 = E_0/Z_0$, with Z_0 being the characteristic impedance in free space), as a further comparison with respect to the incoming wave values. A detailed observation to the internal electromagnetic fields within the dielectric particle confirms also the formation of the anapole mode. In order to mitigate the effect of higher-order multipoles, naturally excited in a stand-alone dielectric particle [21,28,46,62,63], we report in Figs. 5(a)–5(b) the electromagnetic fields for the same dielectric particle with a periodic arrangement as for metamaterials: maps of the absolute value of the electric and magnetic fields intensities are shown, with normalized colorbar to one with respect to the maximum field values.

The electric field map features strong concentration in the center of the cylinder, as in Fig. 4(a) and Fig. 5(a). Additionally, a strong magnetic field forms closed-loop of magnetic field within metamolecule depicted at the same frequency at $f = 1.215\text{ THz}$, as in Fig. 4(b) and Fig. 5(b).

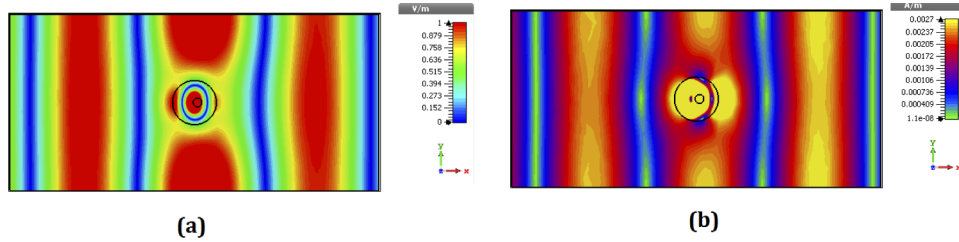


Fig. 4. CST [59] simulation for external electromagnetic fields, with colorbar saturated to $E_0 = 1$ V/m and $H_0 = (120\pi)^{-1}$ A/m. Top view within the stand-alone asymmetric cylindrical particle: normalized (with respect to the maximum value) field maps of (a) absolute value of electric field and (b) absolute value of magnetic field intensities at $f = 1.215$ THz.

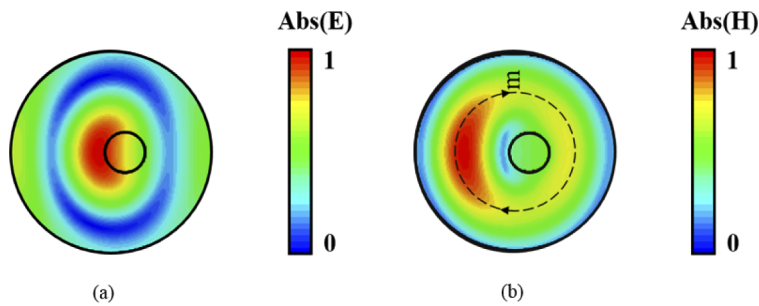


Fig. 5. HFSS simulation [60] for highlighting internal electromagnetic fields, with colorbar normalized to $E_{max} = 1$ V/m and $H_{max} = 1$ A/m. Top view within the asymmetric cylindrical particle: field maps of (a) absolute value of electric field and (b) absolute value of magnetic field intensities (highlighting the formation of loop for the magnetic moment m) at $f = 1.215$ THz.

These fields correspond to anapole state establishment that possesses such strong field localization. In comparison with the plane wave free propagation, the electric field concentration inside the asymmetric cylinder is enhanced up to $E/E_0 = 1.7$ times, while magnetic field concentration is $H/H_0 = 8.2$ times larger than in free space. Such hot-spot fields concentration on the center of the cylinder is a characteristic of the nonradiating anapole mode, accompanied by strong fields in the origin of the metamolecule: in the limit of an infinitesimal anapole mode, electromagnetic fields can be characterized by a Dirac delta function in the origin of the particle [22]. However, in our realistic case for finite size particles, the uncompensated magnetic dipole \vec{M} contribution enlarges the fields around the particles as it can be noticed from Fig. 4(b).

In addition to strong field localization, anapole mode features suppress scattering at the resonance frequency, according to Eq. (15), in terms of multipole decomposition with strongly suppressed total radiation of electric dipole \vec{P} and toroidal dipole \vec{T} moments. According to Fig. 6, the condition $P(f) + ik_0(f)T(f)$ is very close to zero (exact value is 0.000559) at the resonant frequency $f = 1.215$ THz, indicating anapole state formation with almost zero scattering losses. In order to quantitatively validate Eq. (15), we report also the scattering parameter in transmission, together with Eq. (15). The transmission peak around $f = 1.20$ THz in Fig. 6 (red curve) corresponds to the minimum of Eq. (15) in Fig. 6 (black curve), confirming that the total transmission is a result of the suppressed radiation in all directions for the dielectric particle, giving a weak disturbance to the propagation of the incoming electromagnetic field. As expected, the position of the peak is slightly moved with respect to $f = 1.215$ THz due to establishment of uncompensated magnetic dipole \vec{M} in the system.

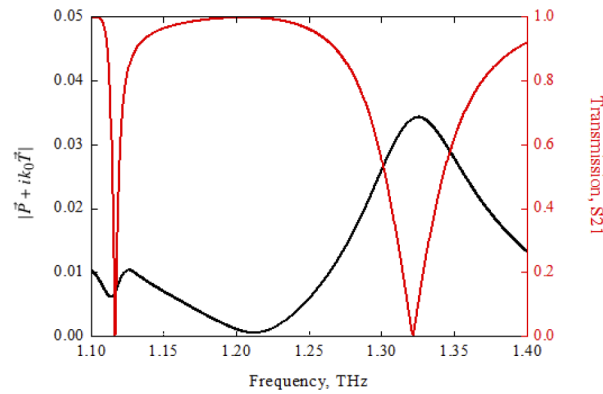


Fig. 6. Total radiation of electric dipole \vec{P} and toroidal dipole \vec{T} moments, i.e. $|\vec{P} + ik_0\vec{T}|$ for hole displacement $d = 3.5\mu\text{m}$ and transmission spectra at resonant frequency close to $f = 1.215$ THz.

By means of this simple and clear example, we show that the symmetry breaking of toroidal metamaterial establishes the anapole mode. Asymmetric configuration of the current distribution creates two oppositely directed current flows \vec{J}_1 and \vec{J}_2 that are responsible for excitation of electric and toroidal dipole modes. At the same time, these currents satisfy Eq. (15), which corresponds to maintain the nonradiating configuration in the anapole state. Apart from the electrodynamics in general, the formalism developed here will be of particular importance for the fields of anapole metamaterials, nanophotonics and invisibility.

We formalize the general approach to the organization of nonradiating sources and scatterers of arbitrary shape. In particular, there exists for any nonradiating configuration always a condition as in Eq. (15) relating two destructively oscillating modes with electric and magnetic origin. This idea can perfectly filled by electric and magnetic anapoles description [20,21,61]. Moreover, symmetry breaking of metaparticles is the second aspect leading to a non-radiating and invisible configuration which currently witness a surge of interest in the properties of transparent systems. Indeed, recently, a numbers of works have already confirmed the key role of anapole excitations in suppression of scattering properties of simple forms, such as all-dielectric nanodisks, clusters and SRR-hybrids [20,21,62,63]. Correspondingly, one may desire to analyze of the electromagnetic response of structurally more complex scatterers for transparency systems. Thus, our approach to asymmetric equivalent current sources could be useful for organizing asymmetrical (electromagnetically) metaparticles of anapole states.

4. Conclusion

In the proposed work, we have first theoretically demonstrated the anapole condition directly from Theorem V of Devaney-Wolf on nonradiating currents, in the framework of volumetric and surface equivalent sources. Consistently with the literature, theoretical results are found in a straightforward manner, relating the polarization \vec{P} to the toroidal dipole vector \vec{T} . In addition, numerical results have shown the existence of the nonradiating anapole mode within a broken-symmetry dielectric particle, a cylindrical object with a hole shifted with respect to the origin in the overall volume V . The proposed approach based on equivalent nonradiating currents turns out to be useful to further explore other types of nonradiating states, higher-order anapole modes, transparent nanophotonics devices and all-dielectric metamaterials.

5. Appendix: Checking purely axial components for multipoles at resonance

Since Eq. (15) relates each vector component separately, in order to estimate the effect of the shifted hole in the dielectric cylinder, we have performed a detailed investigation in a xyz reference system for all the possible excited polarization/magnetization components: this is performed in order to correctly excite purely axial components of electric and toroidal dipoles (for this treatment, the cylinder's axis is directed along the y -axis). With respect to Fig. 2, we have characterized the spectral response of the proposed dielectric metamaterial with respect to the x , y , z strongest axial components for the anapole case in Fig. 3(d), with hole displacement of $d = 3.5\mu\text{m}$. Evidently, the incident wave has polarization vector \vec{E} parallel to cylinder-hole axis and we can expect electric dipole \vec{P} and toroidal dipole \vec{T} to have y -components with negligible x and z intensities. Figure 7 shows the results of simulations for three axial components of each dipole moment in Cartesian coordinate system: P_x, P_y, P_z for electric dipole, M_x, M_y, M_z for magnetic dipole and T_x, T_y, T_z for toroidal dipole moments. As expected, the main contributions at the resonant frequency $f = 1.215$ THz correspond to P_y overlapping the T_y term. The closest contribution to a purely axial dipole-toroidal excitation is the contribution due to the M_x component of the magnetic dipole: however, its value is less than the main dominant P_y - T_y modes for anapole mode formation (up to 1.2 times). Intensities of all other multipoles are suppressed below 10 to 8 times and this is sufficient in order to consider all the other terms negligible contributions.

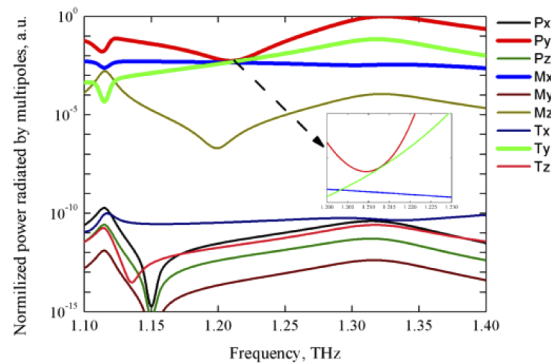


Fig. 7. Normalized power scattered by the multipoles excited in metamolecules at 1.1 THz-1.4 THz frequency range $d = 3.5\mu\text{m}$ hole displacements for three axial components of each dipole moment in Cartesian coordinate system: P_x, P_y, P_z for electric dipole, M_x, M_y, M_z for magnetic dipole and T_x, T_y, T_z for toroidal dipole moments. Inset shows zoom close to $f = 1.215$ THz.

Funding

Compagnia di San Paolo (ANASTASIA project); Deutsche Forschungsgemeinschaft (DFG, German Research Foundation) (Projects SFB/TRR183 and CRC/TRR 191); Ministry of Education and Science of the Russian Federation (K2-2016-051); Russian Foundation for Basic Research (16-02-00789, 16-32-50139); Russian Science Foundation (17-19-01786).

Acknowledgments

The collaboration between Politecnico di Torino (Torino, Italy) and National University of Science and Technology - MISiS (Moscow, Russia) has been possible thanks to the project "Advanced Nonradiating Architectures Scattering Tenuously And Sustaining Invisible Anapoles" (ANASTASIA), funded by Compagnia di San Paolo in the framework of Joint Projects for

the Internationalization of Research. The work of Nikita Nemkov was partially funded by the Deutsche Forschungsgemeinschaft (DFG, German Research Foundation) Projects SFB/TRR183 and CRC/TRR 191. This research work was also partially supported by the Ministry for Education and Science of the Russian Federation, in the framework of the Increase Competitiveness Program of the National University of Science and Technology MISiS under contract number K2-2016-051, the Russian Foundation for Basic Research (Grant Agreements No. 16-32-50139 and No. 16-02-00789). The work on multipoles decomposition investigation of the metamolecules was supported by Russian Science Foundation (project 17-19-01786). In addition, G. Labate and L. Matekovits would like to acknowledge Luca Lussardi for stimulating mathematical discussions and the entire research group of Alexey Basharin for having provided ideal working conditions during their visiting period in Moscow.

References

1. A. Sommerfeld, "Zur elektronentheorie. I. Allgemeine untersuchung des feldes eines beliebig bewegten elektrons," *Akad. der Wiss. (Gott.), Math. Phys. Klasse, Nach.*, 99–130 (1904).
2. A. Sommerfeld, "Zur elektronentheorie. II. Grundlagen fur eine allgemeine dynamik des elektrons," *Akad. der Wiss. (Gott.), Math. Phys. Klasse, Nach.* 363–439 (1904).
3. P. Ehrenfest, "Ungleichformige Elektrizitätsbewegungen ohne Magnet-und Strahlungsfeld," *Physik. Zeit.* **11**, 708–709 (1910).
4. G. A. Schott, "The electromagnetic field of a moving uniformly and rigidly electrified sphere and its radiationless orbits," *Phil. Mag.* **15**(100), 752–761 (1933).
5. G. A. Schott, "The uniform circular motion with invariable normal spin of a rigidly and uniformly electrified sphere, IV," *Proc. Roy. Soc. A* **159**(899), 570–591 (1937).
6. D. Bohm and M. Weinstein, "The self-oscillations of a charged particle," *Phys. Rev.* **74**(12), 1789–1798 (1948).
7. G. H. Goedecke, "Classically radiationless motions and possible implications for quantum theory," *Phys. Rev.* **135**(1B), B281–B288 (1964).
8. A. J. Devaney and E. Wolf, "Radiating and nonradiating classical current distributions and the fields they generate," *Phys. Rev. D* **8**(4), 1044–1047 (1973).
9. K. Kim and E. Wolf, "Non-radiating monochromatic sources and their fields," *Opt. Commun.* **59**(1), 1–6 (1986).
10. M. Berry, J. T. Foley, G. Gbur, and E. Wolf, "A simple explanation of simple non-radiating sources in one dimension comment on nonpropagating string excitations," *Am. J. Phys.* **66**(2), 121–123 (1998).
11. B. J. Hoenders and H. A. Ferwerda, "The nonradiating component of the field generated by a finite monochromatic scalar source distribution," *Pure Appl. Opt.* **7**(5), 1201–1211 (1998).
12. E. Marengo and R. Ziolkowski, "On the radiating and nonradiating components of scalar, electromagnetic, and weak gravitational sources," *Phys. Rev. Lett.* **83**(17), 3345–3349 (1999).
13. B. J. Hoenders and H. A. Ferwerda, "Identification of the radiative and nonradiative parts of a wave field," *Phys. Rev. Lett.* **87**(6), 060401 (2001).
14. G. Gbur, *Nonradiating Sources and the Inverse Source Problem*, University of Rochester Rochester, New York, 2001 (available at: www.maxwell.uncc.edu/gjgbur).
15. A. J. Devaney, "Nonradiating surface sources," *J. Opt. Soc. Am. A* **21**(11), 2216–2222 (2004).
16. G. Gbur, "Nonradiating sources and other invisible objects," Chap. 5 in E. Wolf (Ed.), *Prog. in Optics* (Elsevier, 2003), 273–315.
17. G. Gbur, "Invisibility physics: past, present, and future," *Prog. Opt.* **58**, 65–114 (2013).
18. E. Hurwitz and G. Gbur, "Null-field radiationless sources," *Opt. Lett.* **39**(22), 6529 (2014).
19. F. Monticone and A. Alú, "Embedded Photonic Eigenvalues in 3D Nanostructures," *Phys. Rev. Lett.* **112**(21), 213903 (2014).
20. V. A. Fedotov, A. V. Rogacheva, V. Savinov, D. P. Tsai, and N. I. Zheludev, "Resonant Transparency and Non-Trivial Non-Radiating Excitations in Toroidal Metamaterials," *Sci. Rep.* **3**(1), 2967 (2013).
21. A. E. Miroshnichenko, A. B. Evlyukhin, Y. F. Yu, R. M. Bakker, A. Chipouline, A. I. Kuznetsov, B. Luk'yanchuk, B. N. Chichkov, and Y. S. Kivshar, "Nonradiating anapole modes in dielectric nanoparticles," *Nat. Commun.* **6**(1), 8069 (2015).
22. N. A. Nemkov, A. A. Basharin, and V. A. Fedotov, "Nonradiating sources, dynamic anapole, and Aharonov-Bohm effect," *Phys. Rev. B* **95**(16), 165134 (2017).
23. N. A. Nemkov, I. V. Stenishchev, and A. A. Basharin, "Nontrivial nonradiating all-dielectric anapole," *Sci. Rep.* **7**(1), 1064 (2017).
24. P. C. Wu, C. Y. Liao, V. Savinov, T. L. Chung, W. T. Chen, Y.-W. Huang, P. R. Wu, Y.-H. Chen, A.-Q. Liu, N. I. Zheludev, and D. P. Tsai, "Optical anapole metamaterial," *ACS Nano* **12**(2), 1920–1927 (2018).
25. S.-D. Liu, Z.-X. Wang, W.-J. Wang, J.-D. Chen, and Z.-H. Chen, "High Q-factor with the excitation of anapole modes in dielectric split nanodisk arrays," *Opt. Express* **25**(19), 22375–22387 (2017).

26. J. F. Algorri, D. C. Zografopoulos, A. Ferraro, B. Garcia-Cámara, R. Beccherelli, and J. M. Sánchez-Pena, "Ultrahigh-quality factor resonant dielectric metasurfaces based on hollow nanocuboids," *Opt. Express* **27**(5), 6320–6330 (2019).
27. W. Wang, X. Zhao, L. Xiong, L. Zheng, Y. Shi, Y. Liu, and J. Qi, "Broken symmetry theta-shaped dielectric arrays for a high Q-factor Fano resonance with anapole excitation and magnetic field tunability," *OSA Continuum* **2**(2), 507–517 (2019).
28. N. Papanikolaou, V. A. Fedotov, V. Savinov, T. A. Raybould, and N. I. Zheludev, "Electromagnetic toroidal excitations in matter and free space," *Nat. Mater.* **15**(3), 263–271 (2016).
29. G. N. Afanasiev and Y. P. Stepanovsky, "The electromagnetic field of elementary time-dependent toroidal sources," *J. Phys. A: Math. Gen.* **28**(16), 4565–4580 (1995).
30. G. Labate and L. Matekovits, "Invisibility and cloaking structures as weak or strong solutions of Devaney-Wolf theorem," *Opt. Express* **24**(17), 19245–19253 (2016).
31. A. Alù and N. Engheta, "Achieving transparency with plasmonic and metamaterial coatings," *Phys. Rev. E* **72**(1), 016623 (2005).
32. A. Alù, "Mantle cloak: Invisibility induced by a surface," *Phys. Rev. B* **80**(24), 245115 (2009).
33. U. Leonhardt and T. G. Philbin, *Geometry and Light: The Science of Invisibility* (Dover, 2010).
34. S. Maci, "A Cloaking Metamaterial Based on an Inhomogeneous Linear Field Transformation," *IEEE Trans. Antennas Propag.* **58**(4), 1136–1143 (2010).
35. M. Selvanayagam and G. V. Eleftheriades, "An Active Electromagnetic Cloak Using the Equivalence Principle," *IEEE Ant. and Wireless Prop. Lett.* **11**, 1226–1229 (2012).
36. D. Sounas, R. Fleury, and A. Alù, "Unidirectional Cloaking Based on Metasurfaces with Balanced Loss and Gain," *Phys. Rev. Appl.* **4**(1), 014005 (2015).
37. A. Monti, F. Bilotti, and A. Toscano, "Optical cloaking of cylindrical objects by using covers made of core-shell nanoparticles," *Opt. Lett.* **36**(23), 4479–4481 (2011).
38. P.-Y. Chen and A. Alù, "Mantle cloaking using thin patterned metasurfaces," *Phys. Rev. B* **84**(20), 205110 (2011).
39. E. Shokati, N. Granpayeh, and M. Danaeifar, "Wideband and multi-frequency infrared cloaking of spherical objects by using the graphene-based metasurface," *Appl. Opt.* **56**(11), 3053–3058 (2017).
40. G. Labate, A. Alù, and L. Matekovits, "Surface-admittance equivalence principle for nonradiating and cloaking problems," *Phys. Rev. A* **95**(6), 063841 (2017).
41. G. Labate, S. K. Podilchak, and L. Matekovits, "Closed-form harmonic contrast control with surface impedance coatings for conductive objects," *Appl. Opt.* **56**(36), 10055 (2017).
42. J. B. Pendry, D. Schurig, and D. R. Smith, "Controlling electromagnetic fields," *Science* **312**(5781), 1780–1782 (2006).
43. F. Zolla, S. Guenneau, A. Nicolet, and J. B. Pendry, "Electromagnetic analysis of cylindrical invisibility cloaks and mirage effects," *Opt. Lett.* **32**(9), 1069–1071 (2007).
44. R. G. Quarfoth and D. F. Sievenpiper, "Nonscattering waveguides based on tensor impedance surfaces," *IEEE Trans. Antennas Propag.* **63**(4), 1746–1755 (2015).
45. G. Labate, L. Matekovits, and A. Alù, "Metamaterial and Metasurface Cloaking: Principles and Applications," Chap. 10 in *Surface Electromagnetics (with Applications in Antenna, Microwave, and Optical Engineering)*, F. Yang and Y. Rahmat-Samii, eds., Cambridge University Press, 2019.
46. A. K. Ospanova, G. Labate, L. Matekovits, and A. A. Basharin, "Multipolar passive cloaking by nonradiating anapole excitation," *Sci. Rep.* **8**(1), 12514 (2018).
47. G. Afanasiev and V. Dubovik, "Some remarkable charge-current configurations," *Phys. Part. Nucl.* **29**(4), 366 (1998).
48. A. Ishimaru, *Electromagnetic wave propagation, radiation and scattering* (Prentice-Hall, 1991).
49. J. Van Bladel, *Singular Electromagnetic Fields and Sources*, Chap. 2 (Oxford 1991).
50. C. H. Papas, *Theory of Electromagnetic Wave Propagation* (Dover Publications, Inc., 1965).
51. L. Di Donato, T. Isernia, G. Labate, and L. Matekovits, "Towards Printable Natural Dielectric Cloaks via Inverse Scattering Techniques," *Sci. Rep.* **7**(1), 3680 (2017).
52. C. F. Bohren and D. R. Huffman, (Wiley-Interscience, New York, 1983), 82–84.
53. A. A. Basharin, M. Kafesaki, E. N. Economou, C. M. Soukoulis, V. A. Fedotov, V. Savinov, and N. I. Zheludev, "Dielectric Metamaterials with Toroidal Dipolar Response," *Phys. Rev. X* **5**(1), 011036 (2015).
54. T. Kaelberer, V. A. Fedotov, N. Papanikolaou, D. P. Tsai, and N. I. Zheludev, "Toroidal Dipolar Response in a Metamaterial," *Science* **330**(6010), 1510–1512 (2010).
55. I. V. Stenishchev and A. A. Basharin, "Toroidal response in all-dielectric metamaterials based on water," *Sci. Rep.* **7**(1), 9468 (2017).
56. Y. Fan, Z. Wei, H. H. Chen, and C. M. Soukoulis, "Low-loss and high-Q planar metamaterial with toroidal moment," *Phys. Rev. B* **87**(11), 115417 (2013).
57. Z. Liu, S. Du, A. Cui, Z. Li, Y. Fan, S. Chen, W. Li, J. Li, and C. Gu, "High-Quality-Factor Mid-Infrared Toroidal Excitation in Folded 3D Metamaterials," *Adv. Mater.* **29**(17), 1606298 (2017).
58. Y. Fan, F. Zhang, N.-H. Shen, Q. Fu, Z. Wei, H. Li, and C. M. Soukoulis, "Achieving a high-Q response in metamaterials by manipulating the toroidal excitations," *Phys. Rev. A* **97**(3), 033816 (2018).
59. Microwave Studio, Computer Simulation Technology, 2016.
60. Ansoft High Frequency Structure Simulation (HFSS), Ansoft Corporation, 2016.

61. B. Luk'yanchuk, R. Paniagua-Dominguez, A. I. Kuznetsov, A. E. Miroshnichenko, and Y. S. Kivshar, "Hybrid anapole modes of high-index dielectric nanoparticles," *Phys. Rev. A* **95**(6), 063820 (2017).
62. Y. Yang and S. I. Bozhevolnyi, "Nonradiating anapole states in nanophotonics: from fundamentals to applications," *Nanotechnology* **30**(20), 204001 (2019).
63. K. V. Baryshnikova, D. A. Smirnova, B. S. Luk'yanchuk, and Y. S. Kivshar, "Optical Anapoles: Concepts and Applications," *Adv. Opt. Mater.* **7**(14), 1801350 (2019).